University of Tennessee, Knoxville

TRACE: Tennessee Research and Creative Exchange

Masters Theses

Graduate School

5-2015

Doping of Fluorchlorozirconate and Borate-Silica Glass Ceramics for Medical Imaging and Fast Neutron Scintillation

Julie Elizabeth Swafford
University of Tennessee - Knoxville, jking94@vols.utk.edu

Follow this and additional works at: https://trace.tennessee.edu/utk_gradthes

Part of the Biomaterials Commons, Biomedical Devices and Instrumentation Commons, and the Nuclear Engineering Commons

Recommended Citation

Swafford, Julie Elizabeth, "Doping of Fluorchlorozirconate and Borate-Silica Glass Ceramics for Medical Imaging and Fast Neutron Scintillation. " Master's Thesis, University of Tennessee, 2015.
https://trace.tennessee.edu/utk_gradthes/3414

This Thesis is brought to you for free and open access by the Graduate School at TRACE: Tennessee Research and Creative Exchange. It has been accepted for inclusion in Masters Theses by an authorized administrator of TRACE: Tennessee Research and Creative Exchange. For more information, please contact trace@utk.edu.

www.manaraa.com

To the Graduate Council:

I am submitting herewith a thesis written by Julie Elizabeth Swafford entitled "Doping of Fluorchlorozirconate and Borate-Silica Glass Ceramics for Medical Imaging and Fast Neutron Scintillation." I have examined the final electronic copy of this thesis for form and content and recommend that it be accepted in partial fulfillment of the requirements for the degree of Master of Science, with a major in Biomedical Engineering.

Jacqueline A. Johnson, Major Professor

We have read this thesis and recommend its acceptance:

Dustin Osborne, Justin Baba

Accepted for the Council:
Carolyn R. Hodges

Vice Provost and Dean of the Graduate School

(Original signatures are on file with official student records.)

www.manaraa.com

Doping of Fluorochlorozirconate and Borate-Silica Glass Ceramics for Medical Imaging and Fast Neutron Scintillation

A Thesis Presented for the

Master of Science

Degree

The University of Tennessee, Knoxville

Julie Elizabeth Swafford

May 2015

www.manaraa.com

© by Julie Elizabeth Swafford, 2015
All Rights Reserved.

www.manaraa.com

This is dedicated to my loving family.

www.manaraa.com

Acknowledgments

I would like to acknowledge the University of Tennessee Space Institute and Dr. Jacqueline Johnson for allowing me the opportunity to study and perform research in a field I love.

I would also like to acknowledge Lee Leonard and Carlos Alvarez for their continued guidance and research support,

Acknowledgments also go to David Jacobson at IM2 at neutron beamline at National Institute for Standards and Technology (NIST) and Cai-Lan Wang, Chris Montcalm, and Rick Riedel for fast results at Oak Ridge National Ridge (ORNL).

The National Science Foundation (NSF) is acknowledged for funding this research through grant number DMR 1001381, and Boron for supplying 12B2O3 necessary for neutron scintillation experiments.

www.manaraa.com

"If at first an idea does not sound absurd, then there is no hope for it"

-Albert Einstein

www.manaraa.com

Abstract

Borate silica glass ceramics were produced for neutron scintillation. The Glass ceramics were doped with europium fluoride [EuF_2] and cerium chloride [$CeCl_3$]. Isotopic lithium fluoride [^6LiF] and boron oxide [$^{10}B_2O_3$] were used in most samples while non-isotopic lithium fluoride [LiF] and boron oxide [B_2O3] were used in the rest. When exposed to a neutron beam, samples doped with europium fluoride [EuF_2] scintillated while samples doped with cerium chloride [$CeCl_3$] did not. This contradicts current literature on fast scintillation. What is even more significant is that with europium fluoride [EuF_2] as a dopant, isotopes were not necessary for scintillation results. Eliminating isotopes from the glasses heavily reduces their production cost. This would introduce a high quality, fast scintillator into the market without the expense of isotopes. This has great potential for homeland security, maintenance and safety of nuclear production and storage facilities, and even transportation safety.

ZBLAN glass ceramics were produced for medical imaging. The primary goal was to further investigate crystalline phase transformations of barium chloride [$BaCl_2$]. The phases are important because they determine how the glass ceramic behaves. Hexagonal glasses act as scintillators, orthorhombic phase barium chloride [$BaCl_2$] behave as storage phosphors, and an unknown phase may affect the properties of both. Samples were made and characterized using Differential Scanning Calorimetry, in-situ X-Ray Diffraction, and Phosphorimetry. We found that defects created in the glass ceramics are important to how the crystals form.

www.manaraa.com

Table of Contents

1 Introduction **1**

1.0.1 Fluorochlorozirconate Glasses 1

1.0.2 ZBLAN as a Storage Phosphor 1

1.1 LiSiBaB Glass Ceramics Scintillators 2

1.1.1 Current use of Borate Glasses 2

1.1.2 Need for Fast Scintillators 2

1.1.3 Applications of LiSiBaB Scintillators 3

2 Materials and Methods **4**

2.1 Glass Ceramics for Medical Imaging 4

2.1.1 Sample Preparation 4

2.1.2 Glass Synthesis 4

2.1.3 Annealing Samples to Glass Ceramics 7

2.1.4 Differential Scanning Calorimetery 9

2.1.5 X-Ray Diffraction 11

2.1.6 Phosphorimetry 12

2.2 LiSiBaB Glass Ceramics for Fast Neutron Scintillation 12

2.2.1 Sample Preparation 12

2.2.2 Glass Synthesis 15

2.2.3 Annealing Samples to Glass Ceramics 17

2.2.4 Testing At NIST 17

www.manaraa.com

2.2.5 Testing At ORNL 18

3 Results **22**

3.1 ZBLAN Glasses 22

3.1.1 Differential Scanning Calorimetry (DSC) 22

3.1.2 In-situ X-ray Diffractometry 26

3.1.3 Phosphorimetry (PL) 28

3.2 Borate Scintillators 28

3.2.1 NIST exposure 28

3.2.2 Pulse Height Measurements 33

3.2.3 Pulse Shape Measurements 35

4 Conclusions **39**

4.1 ZBLAN Glass Ceramics 39

4.1.1 Future Work 40

4.2 LiSiBaB Glass Ceramics 40

4.2.1 Future Work 41

Bibliography **42**

Vita **45**

www.manaraa.com

List of Tables

2.1 Table depicting the sample compositions in mole percent 6

2.2 Table depicting the neutron scintillator sample compositions in mole percent 16

3.1 Table detailing at which temperature/time each phase developed when heated at 10°C/minute 27

3.2 Table detailing at which temperature/time each phase developed when heated isothermally at 305°C 27

3.3 Table detailing the temperature/time each phase developed when held at 315°C 27

www.manaraa.com

List of Figures

2.1 MBraun LABmaster glovebox 5
2.2 Furnace program for samples production 8
2.3 Mold temperature program for sample cooling 8
2.4 Set up for sample pre-heat treatments 9
2.5 Aluminum boat that holds sample during heat treatments 10
2.6 Set up for heat treatments in tube furnace 10
2.7 Netzsch DSC 11
2.8 DSC chamber 12
2.9 Philips X'Pert XRD 13
2.10 XRD stage with aluminum peg 14
2.11 Setup of PL used in sample characterization 14
2.12 Furnace program for LiSiBaB production 17
2.13 System Schematic for NIST neutron imaging apparatus 19
2.14 NIST powdered sample setup 20
2.15 Schematic of PG-PHS used in sample characterization 20
2.16 Illustration of PH system used in sample characterization 21

3.1 DSC scans for all of the FCZ glass samples made this year prior to in-situ x-ray heat treatments. The data are stacked for clarity 23
3.2 DSC scans for FCZ glass samples including previously made and characterized samples JJ176 and JJ177 24

www.manaraa.com

3.3 DSC close up of FCZ glasses for clarity of hexagonal and bulk crystalline phases. The orthorhomibic $BaCl_2$ phase can be seen here in JJ176 and JJ177 around 295°C 25
3.4 Isothermal DSC scans of FCZ glasses 26
3.5 Excitation Spectra for previously made FCZ glasses containing 1.2% EuF_2, 0.8% HoF_3 (JJ124) and 0.8%$EuCl_2$ (JJ176). Samples were excited at 545 nm. 29
3.6 Excitation Spectra for FCZ glasses containing 1.5% $EuCl_2$, 1.5% HoF_3 (JJ204) and 3%HoF_3 (JJ206). Samples were excited at 545 nm. . . . 29
3.7 Excitation Spectra of samples JJ124, JJ176, JJ204, and JJ206. Samples are stacked for clarity. Samples were excited at 545 nm. . . . 30
3.8 Figure 7: Emission spectra for FCZ glasses containing 0.8% EuF_3, 1.2%EuF_2 (JJ124), 0.8% $EuCl_2$ (JJ176), and 0.8% $EuCl_2$, 1.2% HoF_3 (JJ177). The samples were excited at 360 nm. 30
3.9 Emission spectra for FCZ glasses containing 1.5% $EuCl_2$, 1.5% HoF_3 (JJ204), and 3% $EuCl_2$ (JJ205). The samples were excited at 360 nm. 31
3.10 Emission spectra for samples JJ124, JJ176, JJ177, JJ204, and JJ205. The samples were excited at 360 nm. The samples were stacked for clarity. 31
3.11 Neutron scintillation of "as made" samples 32
3.12 Neutron scintillation of powdered LiSiBaB samples 33
3.13 Pulse height measurement of sample JJ221 34
3.14 Pulse height measurement of the commercial standard GS20 34
3.15 Pulse height measurement of sample JJ222 35
3.16 Pulse height measurement of sample JJ223 36
3.17 Pulse height measurement of sample JJ224 36
3.18 Pulse height measurement of sample JJ225 37
3.19 Pulse height measurement of sample JJ226 37
3.20 Pulse shape measurement of sample JJ221 38

www.manaraa.com

3.21 Pulse shape measurement of commercial standard GS20 38

www.manaraa.com

Chapter 1

Introduction

1.0.1 Fluorochlorozirconate Glasses

Fluorochlorozirconate (FCZ) glasses have been researched and developed since its discovery in 1975. The original composition contained 50% ZrF_4, 25% BaF_2, and 25% NaF; this has been modified to achieve various specific glass properties. Research and development with FCZ glasses have led to the development of ZBLAN (which is acronymed from it's composition of ZrF_4, BaF_2, LaF_3, AlF_3, and NaF) [Poulain and Soufiane (1992)].

1.0.2 ZBLAN as a Storage Phosphor

ZBLAN glass ceramics have a lower photon energy, and thermal treatments [Pablick (2010)] cause specific nanocrystalline phases to develop [Pfau (2011)] in them. Mauro and Zanotto (2014) challenged researchers to increase research and the development of glasses that can be used to fight disease and improve human health. Using doped ZBLAN as a storage phosphor in place of current film systems could achieve this goal.

In order to further the research Mauro has called upon, ZBLAN glass ceramics were further investigated as a storage phosphor plate. $BaCl_2$ replaced BaF_2 in the standard ZBLAN formula. This was done to achieve the orthorhomibic $BaCl_2$

www.manaraa.com

phase needed to create a storage phosphor[Schweizer (2001)]. The orthorhombic and hexagonal $BaCl_2$ crystalline phases occur when Eu^{2+} is also present. An increase in $BaCl_2$ crystals precipitated during heat treatments seem to be caused by the addition of HoF_3 [Gray (2013)].

1.1 LiSiBaB Glass Ceramics Scintillators

1.1.1 Current use of Borate Glasses

Borate glasses using orthorhombic $BaCl_2$ nanocrystallites and dEu^{2+} as a dopant have been proven to work as a storage phosphor, much like our previous work with ZBLAN or x-ray imaging. Borate-lithium:Eu^{2+} glass ceramics have been created as neutron imaging plates. The use of Eu^2 and orthorhombic $BaCl_2$ nanocrystallites have given rise to PSL. The BaFBr:Eu^{2+} glass ceramics have good performance in key readout characteristics, such as resolution, sensitivity, and dynamic range, when compared to commercially available Fujifilm powder plates [Appleby et al. (2005)].

When the LiBBaCl glass ceramics mentioned above are irradiated with thermal neutrons, the ^{10}B and ^{6}Li produce secondary alpha particles. These secondary alpha particles create electron-hole pairs which generate F-centres. The recombination of these electron-hole pairs gives a blue photostimulated luminescence (PSL) emission [Appleby and Vontobel (2008)]. This is similar to how the ZBLAN glass ceramic storage phosphor plates, that are familiar with making, behave. Applying our experience to the borate glass ceramic matrix might yield novel results.

1.1.2 Need for Fast Scintillators

Throughout the fields of high-energy physics and nuclear medicine, the search for a new scintillators has been a constant research topic. CeF_3 was developed for this purpose in the late 1980's. Large crystals of Ce^{3+} were developed as a possible fast

www.manaraa.com

scintillator, and it is still the main dopant of choice for fast scintillation [Anderson (1990)].

1.1.3 Applications of LiSiBaB Scintillators

Inorganic scintillators are the most widely used scintillator types in medical diagnostic imaging modalities that use x-rays or gamma rays. Because each diagnostic method is different, the properties of their respective scintillators must also be different. This, along with the development of new imaging systems, is why research on scintillators is still being done. An ideal LiSiBaB scintillator could replace current scintillators used in X-ray imaging, X-ray computed tomography(CT), single-photon computer radiography (SPECT), and positron emission tomography (PET). Research in Ce^{3+} ceramic scintillators is where investigation has been focused [Carel (2002)].

www.manaraa.com

Chapter 2

Materials and Methods

2.1 Glass Ceramics for Medical Imaging

2.1.1 Sample Preparation

Samples were produced in an MBraun LABmaster SP glovebox with an OTF-1200-2 dual zone tube furnace attached (see Figure 2.1). Both of these were pumped with argon gas continually. This provided an inert argon atmosphere for glass production and chemical storage in which the oxygen and moisture were controlled and monitored. Water and oxygen levels consistanly remained below 0.1 ppm.

2.1.2 Glass Synthesis

Eleven different compositions of fluorochlorozirconate glass samples were produced to make up a series. The series varied in the amount of ZrF_4, $EuCl_2$, EuF_2, EuF_3, and HoF_3. Ten gram samples of each composition were made in the glovebox furnace combination mentioned above. Table 2.1 shows the different compositions used.

www.manaraa.com

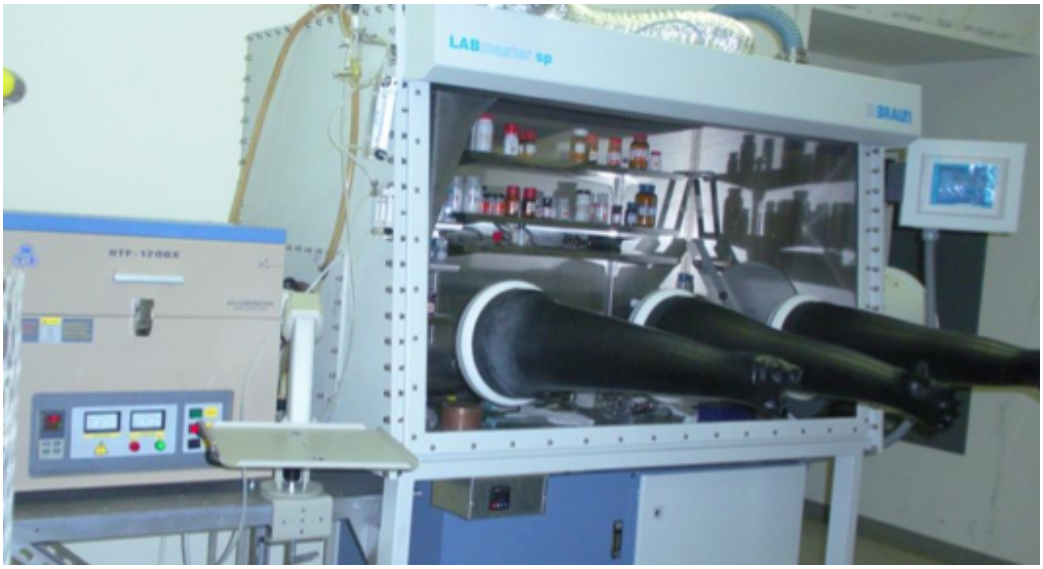

Figure 2.1: MBraun LABmaster glovebox used to produce samples

www.manaraa.com

Table 2.1: Table depicting the sample compositions in mole percent

Sample	ZrF_4	$BaCl_2$	NaF	AlF_3	LaF_3	InF_3	$EuCl_2$	HoF_3	EuF_2	EuF_3	B_2O_3
JJ194	51	20	20	3	3.5	0.5	0	0	2	0	0
JJ195	51	20	20	3	3.5	0.5	0	0	0	2	0
JJ196	52.3	20	20	3	3.5	0.5	0.8	0	0	0	0
JJ197	51	20	20	3	3.5	0.5	0.8	1.2	0	0	0
JJ198	51	20	20	3	3.5	0.5	0	1.2	0.8	0	0
JJ199	51	20	20	3	3.5	0.5	0	1.2	0	0.8	0
SG004	51.2	20	20	3	3.5	0.5	0.8	0	0	0	1
JJ228	48	20	20	3	3.5	0.5	0.8	4.2	0	0	0
JJ227	49	20	20	3	3.5	0.5	0.8	3.2	0	0	0
SG003	50	20	20	3	3.5	0.5	0.8	2.2	0	0	0
JJ229	50	20.94	20.94	3.14	3.66	0.52	0.8	0	0	0	0

www.manaraa.com

The samples were produced using a two step process. Chlorides tend to evaporate at higher temperatures, so the fluorides were melted in the first step. The fluoride powders were measured into a platinum crucible, covered with a platinum lid, and inserted into the tube furnace.

The powders went through a one hour drying phase at 400°C. The furnace temperature was increased at 10°/minute to 800°C. The powders were held at 800°C for one hour for melting, then taken out to add the chlorides. The chloride powders were measured into the crucible, covered, and placed back into the tube furnace at 750°C. The melt remained at 750° for one hour then decreased at 10°/minute to 700° where it stayed for ten minutes. Figure 2.2 is an image detailing the temperature program described above. The crucible was removed from the furnace and the melt was poured into a brass mold pre-heated to 200°C right below the glass transition temperature, which prevents crystallization. The mold slowly cools down to room temperature (25°C) over four hours in a controlled manner; Figure 2.3 shows the cooling ramp. The glass is then taken out of the mold and cut for characterization and heat treatments. When not being studied, the samples were stored in a desiccator to prevent atmospheric contamination.

2.1.3 Annealing Samples to Glass Ceramics

Heat treatments of the glass samples were done by two different methods. Firstly, they were treated using a hot plate; this setup is depicted in Figure 2.4. The samples were cut in centimeter squares and placed inside an aluminum boat that rested on the hot plate. The samples were held within two degrees of the target temperature for five minutes. The second method for heat treatments was also applied to 1 cm^2 samples. The samples were placed in an aluminum "boat" that held the sample in the tube furnace; the "boat" is depicted in Figure 2.5. The sample stayed in the tube furnace for five minutes at the target temperature +/- 2°C. The setup for the tube furnace heat treatment is presented in Figure 2.6. Prior to the

www.manaraa.com

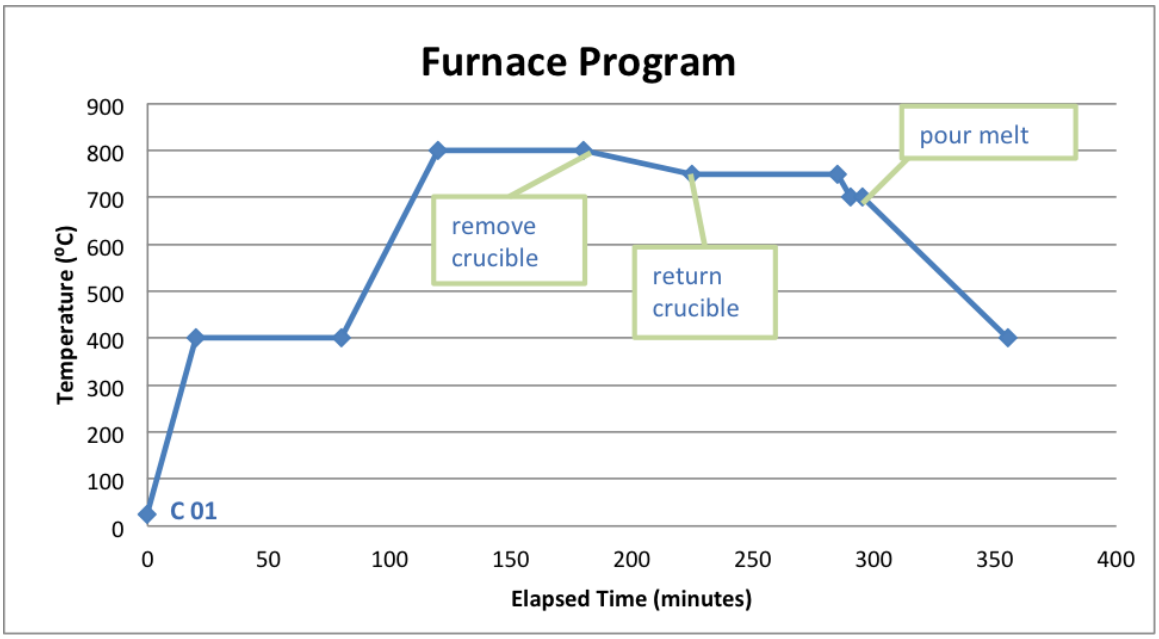

Figure 2.2: Furnace program for samples production

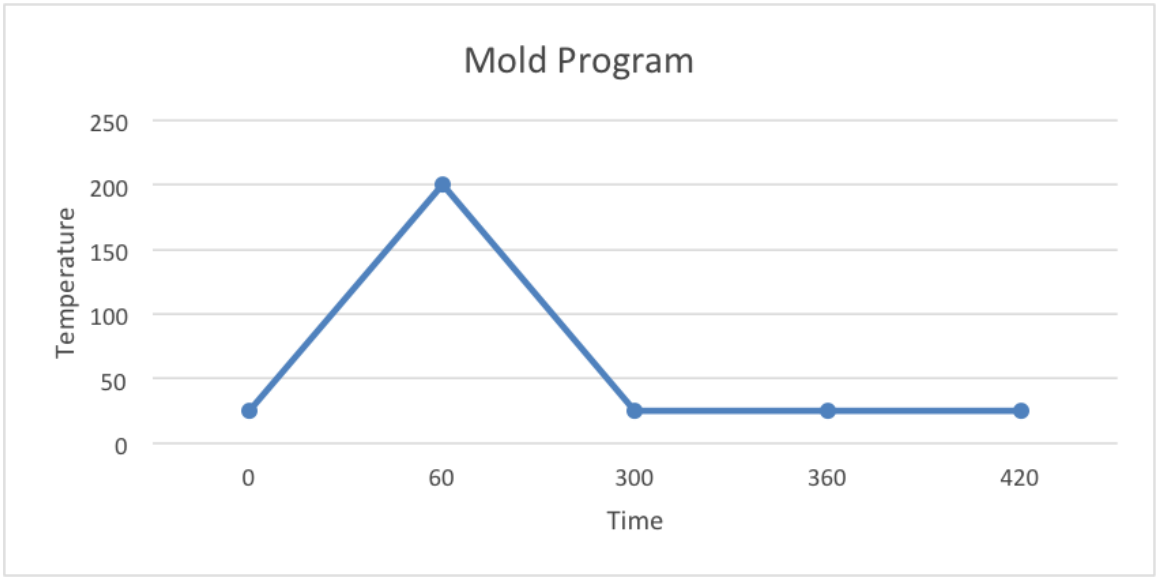

Figure 2.3: Mold temperature program for sample cooling

www.manaraa.com

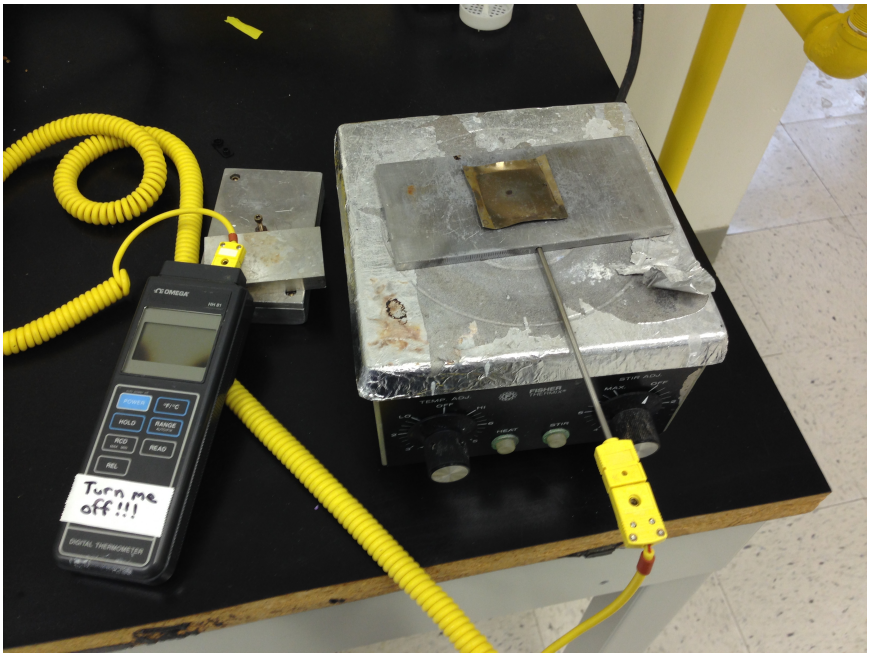

Figure 2.4: Set up for sample pre-heat treatments

heat treatments, the samples were pre-heated at 200°C for 5 minutes. Hexagonal and orthorhombic (when applicable) inducing temperatures were used to treat each sample. The temperatures for the heat treatments were determined by differential scanning calorimetry experiments.

2.1.4 Differential Scanning Calorimetery

Differential Scanning Calorimetry (DSC) was used to find the glass transition temperature (Tg° and crystallization temperatures (Tx°). A Netzsch DSC 200F3 was used for these measurements. This instrument is depicted in Figure 2.7. Proteus Thermal Analysis Software (Version 5.2.1) was used to analyze the spectra to accurately determine Tg° and Tx°.

Aliquots were taken from the interior of the "as-poured" samples at weights of ten to thirty grams. Each aliquot was placed in the Netzsch aluminum crucible and sealed with an aluminum lid. The samples were placed in the DSC chamber shown

www.manaraa.com

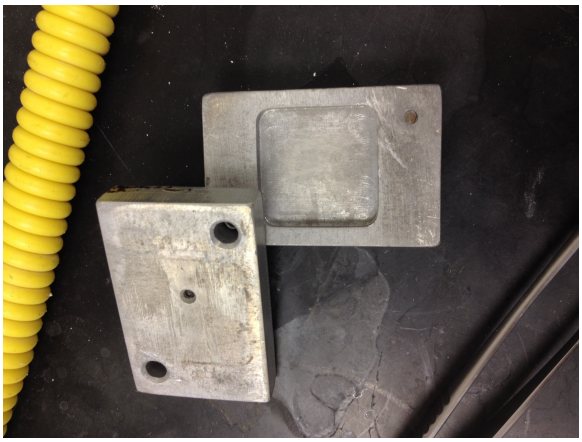

Figure 2.5: Aluminum boat that holds sample during heat treatments

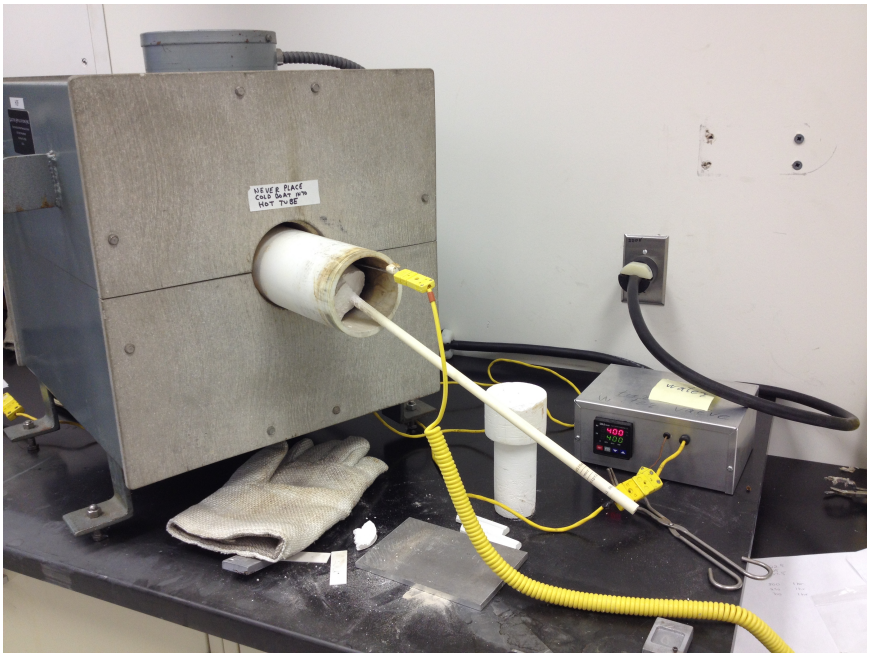

Figure 2.6: Set up for heat treatments in tube furnace

www.manaraa.com

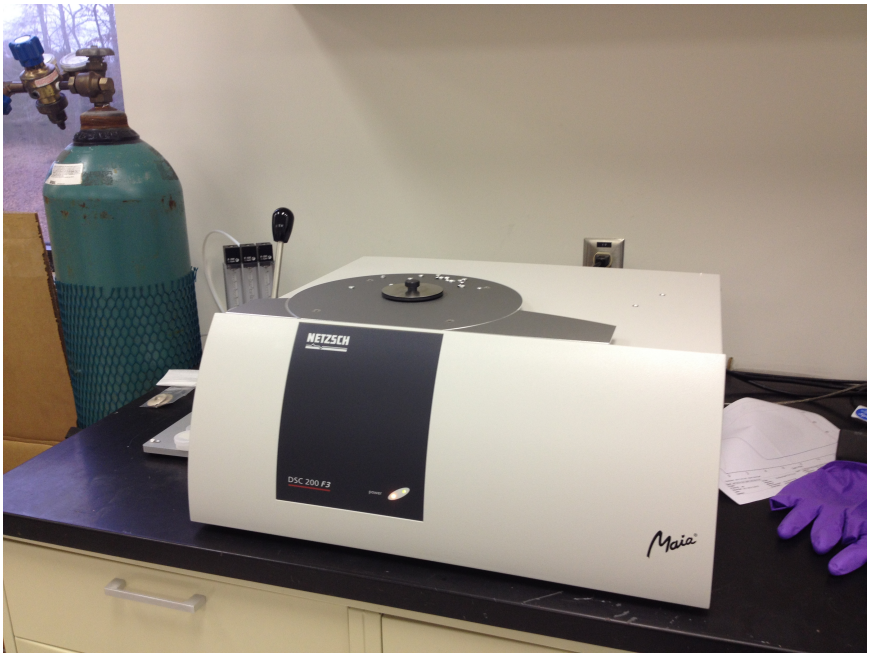

Figure 2.7: The Netzsch DSC used for sample phase characterization

in Figure 2.8, which was purged with 40 milliliters per minute of nitrogen during the scans. The samples were heated from 100°C to 500° at 10°C per minute.

2.1.5 X-Ray Diffraction

Samples were tested using X-Ray diffraction (XRD), to determine the crystallization phases in each sample. The previously heat treated samples were polished to reveal the bulk glass. The characterization was performed using a Philips X'Pert XRD depicted in Figure 2.9. The samples were attached to an aluminum peg located on the stage of the XRD with double sided tape; this is seen in Figure 2.10. Measurements were taken using a step size of $0.5°\theta$ with a ten second step time from twenty to eighty two theta degrees. MDI Jade 9 software was used to analyze the results and determine the specific crystallization phases for each sample. The samples were compared to diffraction pattern files in Jade.

www.manaraa.com

Figure 2.8: A birds eye view inside of the DSC chamber where the samples were placed

2.1.6 Phosphorimetry

Phosphorimetry (PL) was performed on the heat treated samples to confirm the crystalline phases in each of the samples. A PTI QM30 model 810/814 photomultiplier detection system and XenoFlash were used to acquire these measurements. Figure 2.11 shows the system set up for this characterization test. A xenon lamp, with a diffraction grating, exposed the samples to wavelengths corresponding to their dopants and recorded their emission. FeliX32 software was used to analyze the results.

2.2 LiSiBaB Glass Ceramics for Fast Neutron Scintillation

2.2.1 Sample Preparation

Samples were produced in the same environment as the ZBLAN glass ceramics mentioned previously. The samples were made in an MBraun LABmaster SP glovebox with an OTF-1200-2 dual zone tube furnace attached (see Figure 2.1) that was purged continuously with argon gas. Water and oxygen levels consistanly remained below 0.1 ppm.

www.manaraa.com

Figure 2.9: Philips X'Pert XRD

www.manaraa.com

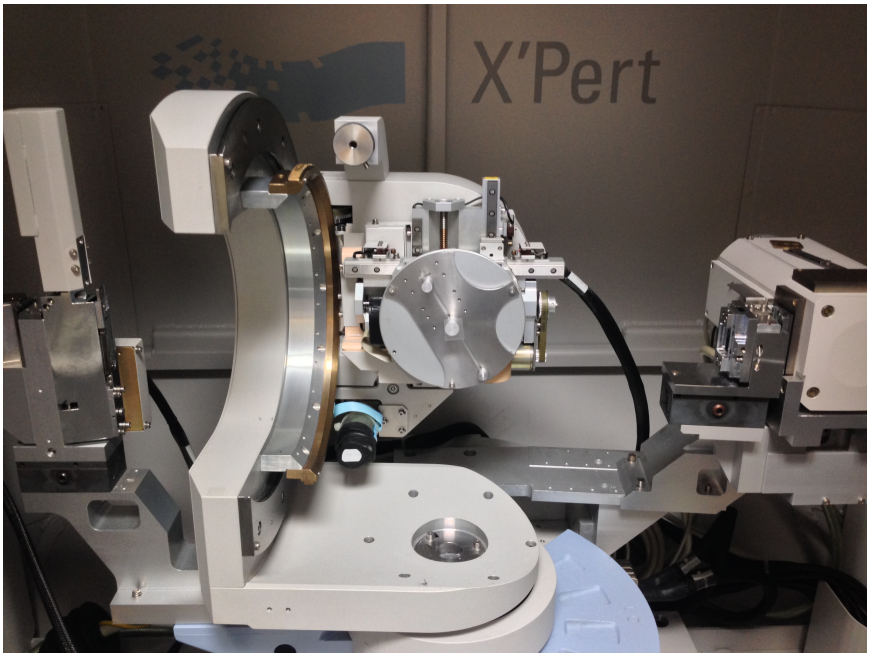

Figure 2.10: XRD stage with aluminum peg

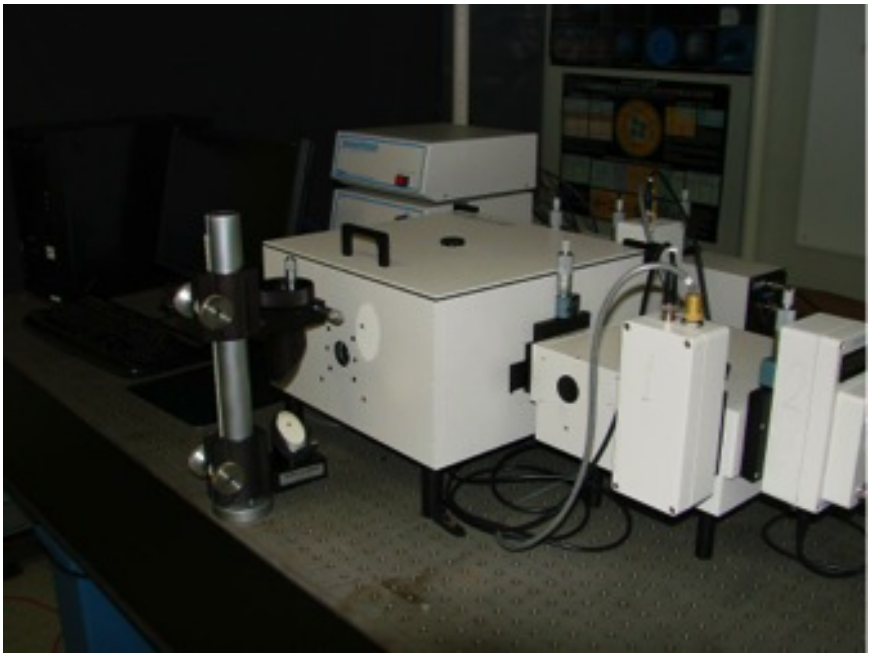

Figure 2.11: Setup of PL used in sample characterization

www.manaraa.com

2.2.2 Glass Synthesis

Six different compositions of doped LiSiBaB glass samples were produced to make up the series. 10 gram samples of each composition were made in the glovebox furnace. Table 2.2 shows the different compositions used. Figure 2.12 shows the temperature program used to synthesize the glasses.

www.manaraa.com

Table 2.2: Table depicting the neutron scintillator sample compositions in mole percent

Sample	B_2O_3	$^{10}B_2O_3$	Li_2O	LiF	^6LiF	$BaCl_2$	BaF_2	$CeCl_3$	CeF_3	EuF_2	SiO_2
JJ221	50	0	25	5	0	15	0	1	0	0	4
JJ222	50	0	25	5	0	15	0	0	0	1	4
JJ223	0	50	25	0	5	15	0	0	0	1	4
JJ224	0	50	25	0	5	0	15	0	0	1	4
JJ225	0	50	25	0	5	15	0	0	1	0	4
JJ226	0	50	25	0	5	0	15	0	1	0	4

www.manaraa.com

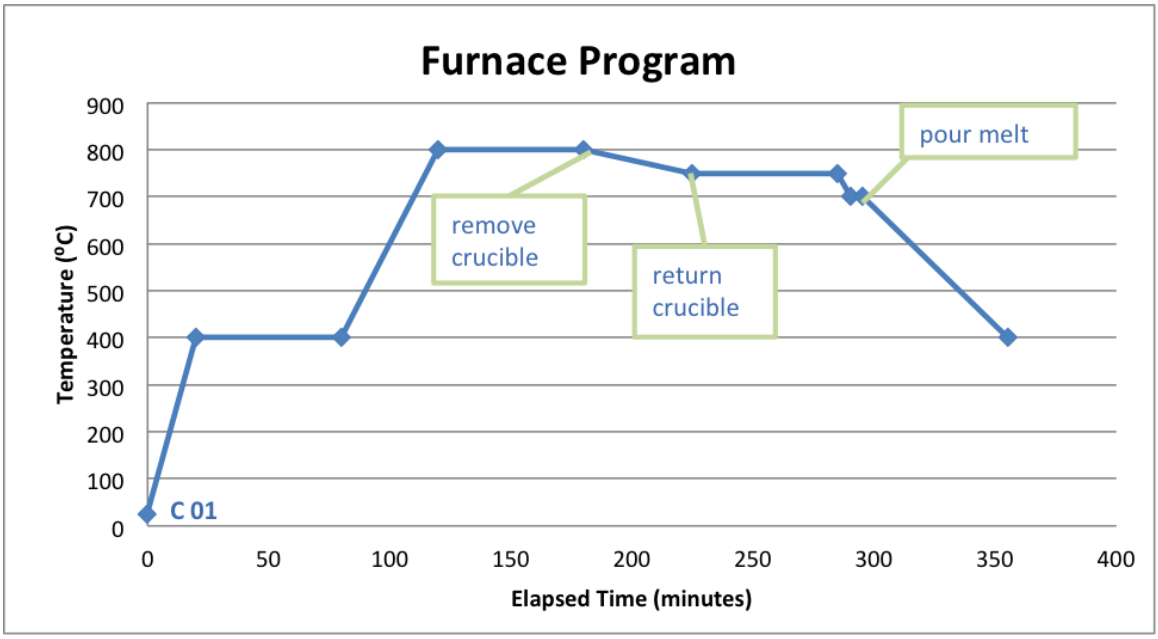

Figure 2.12: Furnace program for LiSiBaB production

The samples were produced in one step. The powders were weighed into a platinum crucible, covered with a platinum lid, and inserted into the tube furnace. The crucible was removed from the furnace and the melt was poured into a brass mold pre-heated to 200°C just below the glass transition temperature; this prevented crystallization. The mold was slowly cooled down to room temperature (25°C) over four hours in a controlled manner. The glass was then taken out of the mold and cut for characterization and heat treatments. When not being studied, the samples were stored in a desiccator to prevent atmospheric contamination.

2.2.3 Annealing Samples to Glass Ceramics

LiSiBaB samples were annealed into a glass ceramic during the synthesis process.

2.2.4 Testing At NIST

Images were taken at NIST using the apparatus shown in Figure 2.13. Item 1 in Figure 2.13 is the point source of neutrons. Item 2 is the neutron to light converter.

www.manaraa.com

Item 3 is the first 45° surface mirror. Item 4 is a light tight box. Item 5 is a standard camera lens. Item 6 is a CMOS image sensor, and Item 7 is the computer for image analysis.

1.5mm "as made" samples were secured to an aluminum sample holder plate using double sided tape. The samples and sample holder were placed in the line of sight of the neutron source. "As made" samples were then powdered using a mortar and pestle. The powdered samples were attached to the sample holder using double sided tape. Clear packaging tape was placed over the samples to hold the powders in place; this can be seen in Figure 2.14.

The neutrons were exposed to the scintillator samples. Light emitted from the samples was reflected off the first surface mirror and focused on to the CMOS image sensor. The computer collected the data received from the sensor. Dark images were taken to process the transmission images. The images were analyzed using an image analysis software program written by NIST beam-line scientists.

2.2.5 Testing At ORNL

Gated Pulse Height Spectra

G-PHS determines photons per thermal neutron. Gated pulse height spectra (G-PHS) characterizations were performed on the scintillator samples at Oak Ridge National Lab (ORNL) after imaging at NIST. It is integrated at the peak channels to determine this amount. Cf^{252} and Co^{60} were used as sources for this experiment. A GS20 commercial standard was tested for comparison; it is 1.5mm thick of 6.6% enriched ^{6}LiF.

Pulse shape measurements were made to aid in discrimination between neutrons and gammas. Cf^{252} was used as the neutron source and Co^{60} as the gamma source. Again, a commercial standard (GS20) was tested for comparison.

www.manaraa.com

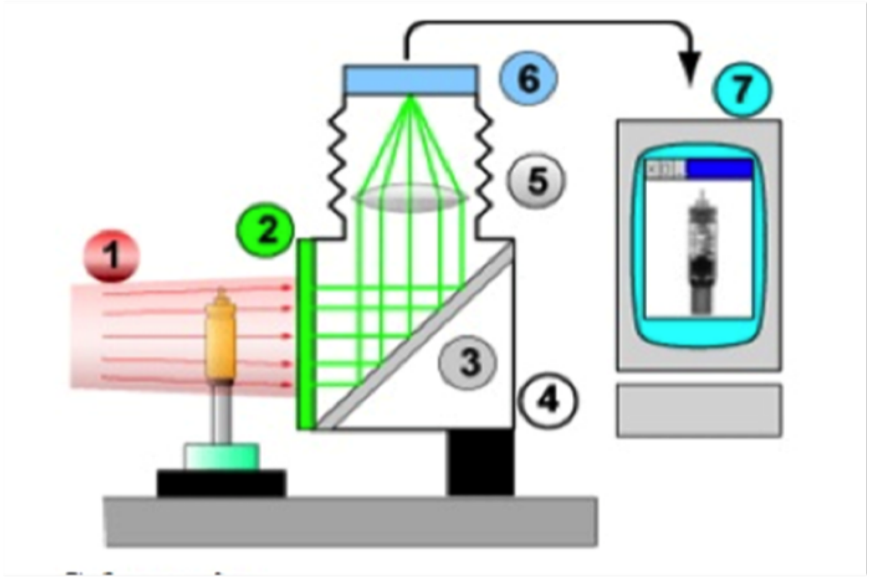

Figure 2.13: System Schematic for NIST neutron imaging apparatus

www.manaraa.com

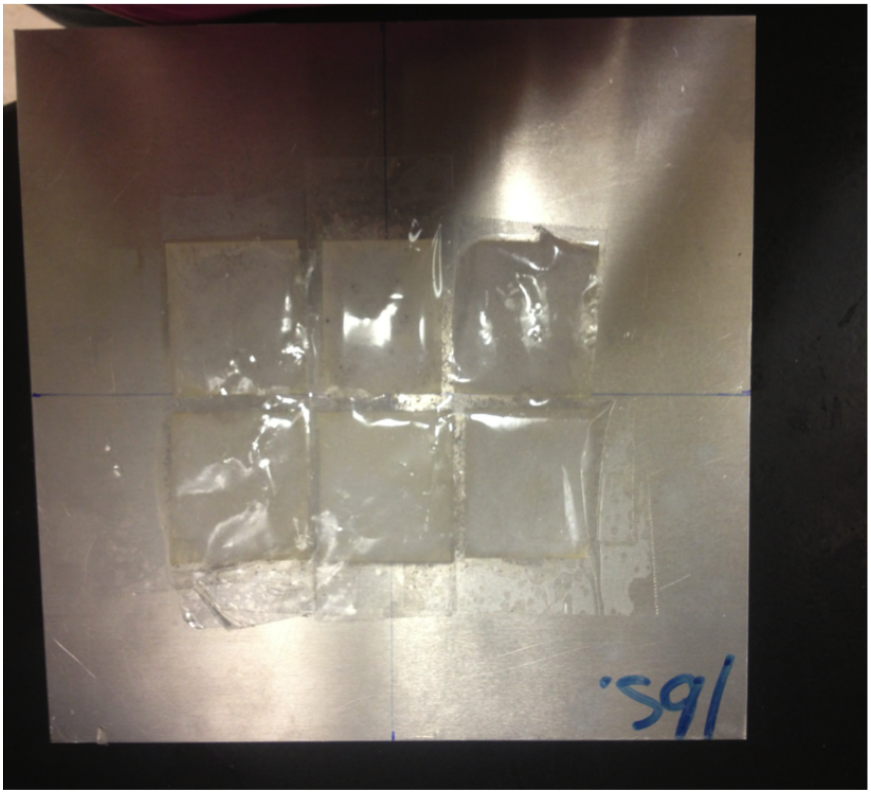

Figure 2.14: Powdered samples arranged on a aluminum plate for exposure and imaging

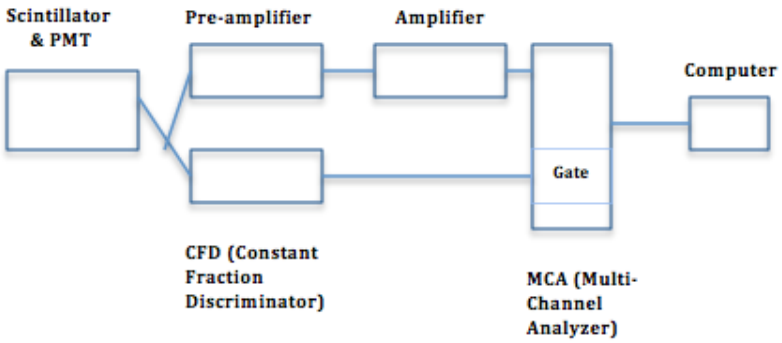

Figure 2.15: Schematic of PG-PHS used in sample characterization

www.manaraa.com

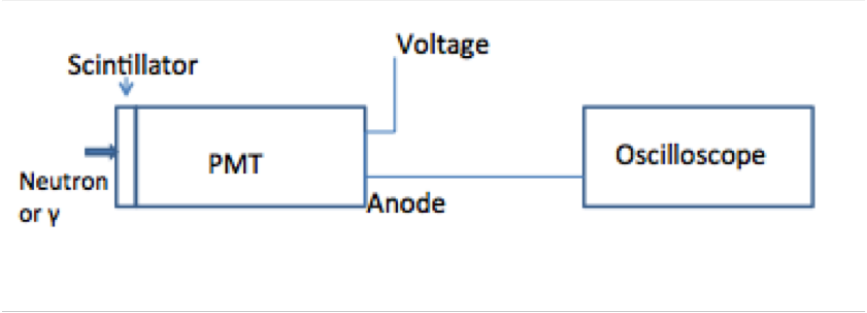

Figure 2.16: Illustration of PH system used in sample characterization

Here the scintillator samples were exposed to gamma and neutrons sources, and the light pulses were recorded by an oscilloscope. A diagram of the apparatus is presented in Figure 2.16.

www.manaraa.com

Chapter 3

Results

3.1 ZBLAN Glasses

3.1.1 Differential Scanning Calorimetry (DSC)

DSC scans were done on each of the glass samples prior to any type of heat treatment or other characterization. Below in Figure 3.1 are the DSC results; they are stacked for comparison. The results are consistent with $BaCl_2$ crystalline formations. The first dip in the scans indicates the glass transition phase. The first exothermal peak is indicative of hexagonal phase $BaCl_2$, and it occurs around 250°C. The second exothermal represents the orthorhombic phase of $BaCl_2$, and they occur at 300°C (+/- 5°C). The third exothermal peak is a result of the crystallization of the bulk glass matrix. Samples doped with $EuCl_2$ usually have a higher bulk crystallization temperature with HoF_3 doped samples crystallizing at an even higher temperature.

ZBLAN glass ceramic samples usually have a distinctive second exothermal peak that is representative of the orthorhombic $BaCl_2$ phase formation. Most samples in this series do not have the second exothermal peak. Because glass matrices require defects in order for the $BaCl_2$ crystals to form, the nonexistent second exothermal peak could be caused by a lack of defects.

www.manaraa.com

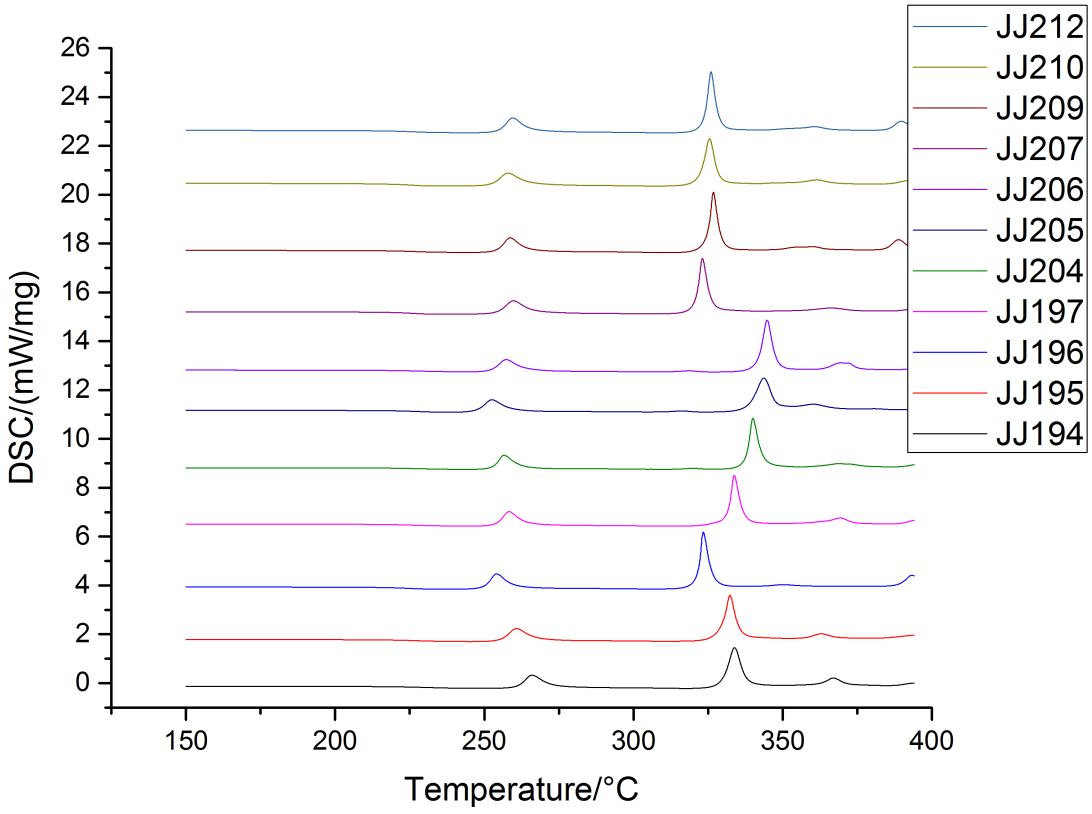

Figure 3.1: DSC scans for all of the FCZ glass samples made this year prior to in-situ x-ray heat treatments. The data are stacked for clarity

www.manaraa.com

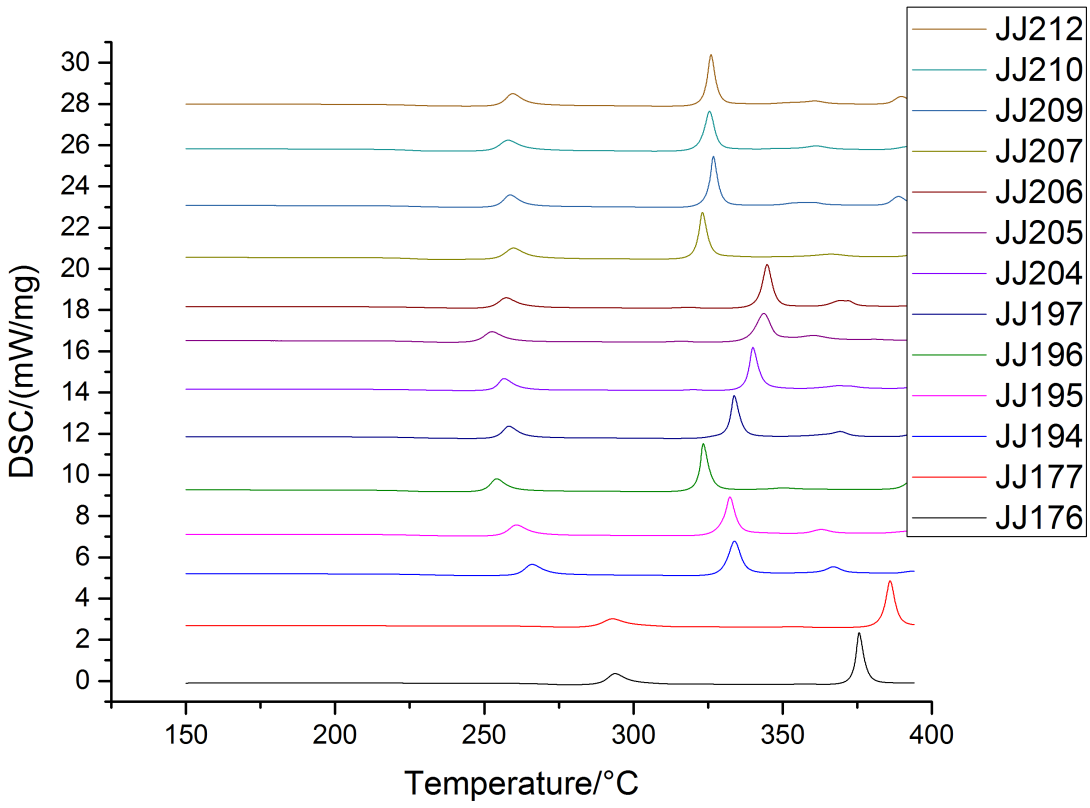

Figure 3.2: DSC scans for FCZ glass samples including previously made and characterized samples JJ176 and JJ177

www.manaraa.com

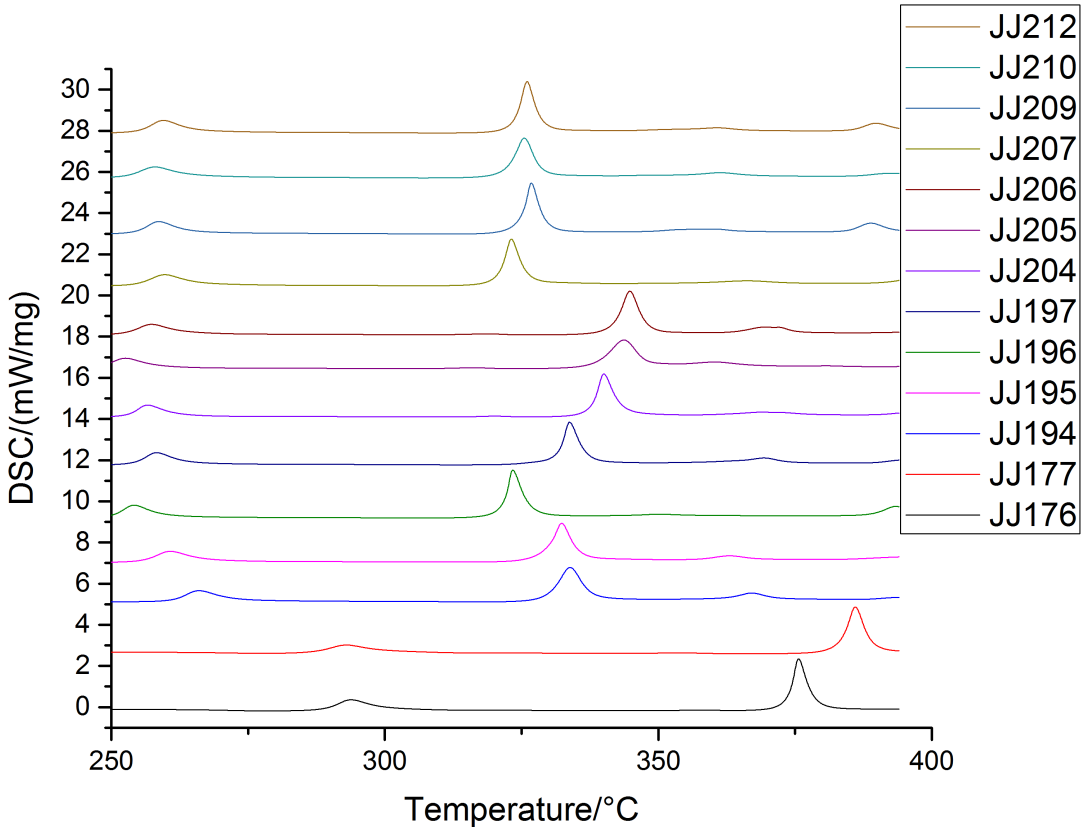

Figure 3.3: DSC close up of FCZ glasses for clarity of hexagonal and bulk crystalline phases. The orthorhomibic $BaCl_2$ phase can be seen here in JJ176 and JJ177 around 295°C

www.manaraa.com

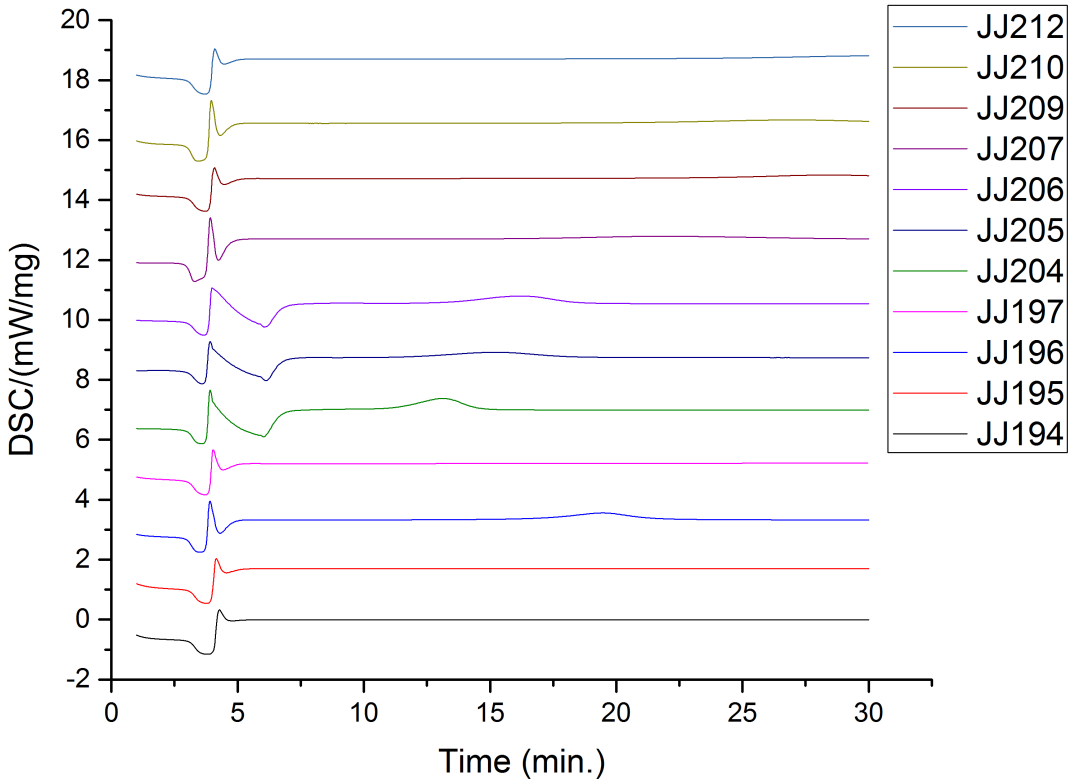

Figure 3.4: Isothermal DSC scans of FCZ glasses

Isothermal DSC scans were run on the samples to see if an orthorhombic crystalline phase would develop after prolonged heating. JJ196 and JJ208 developed orthorhombic crystalline peaks at 19 and 23 minutes when held at a temperature of 300°C.

3.1.2 In-situ X-ray Diffractometry

In-situ X-ray diffractometry (XRD) performed at the DND-CAT facilities at Argonne National Lab yielded several sets of results for the FCZ samples. Table 3.1, Table 3.2, and Table 3.3 show samples heated at 10°C per minute, isothermally at 305°C, and isothermally at 315° respectively. Table 3.1 gives the temperature (°C)/time (min) at which the phase listed develops. Table 3.2 gives the temperature (°C)/time (min)

www.manaraa.com

Table 3.1: Table detailing at which temperature/time each phase developed when heated at 10°C/minute

Sample	Hexagonal $BaCl_2$	Orthorhombic $BaCl_2$	Unknown Phase
JJ194	264/12	-	324/25
JJ195	260/11	325/29	335/26
JJ196	255/11	315/23	325/25
JJ197	225/9	315/21	335/25
JJ198	264/12	324/24	-
JJ199	225/10	320/23	330/25

Table 3.2: Table detailing at which temperature/time each phase developed when heated isothermally at 305°C

Sample	Hexagonal $BaCl_2$	Orthorhombic $BaCl_2$	Unknown Phase
JJ194	292/3	-	-
JJ195	225/3	-	-
JJ196	240/3	-	305/19
JJ197	248/3	-	-
JJ198	272/4	-	-
JJ199	296/5	-	-

at which the phases developed when held at 305°C. Table 3.3 gives the temperature (°C)/time (min) at which the phase listed developed when held at 315°C.

It is always true that the hexagonal $BaCl_2$ phase develops prior to the orthorhombic and unknown phases. Note that in some samples the orthorhombic phase develops before the unknown phase (samples JJ196, JJ197, and JJ199), but the reverse was true in others (namely samples JJ194, JJ195, and the 315°C isotherm of JJ197). Samples

Table 3.3: Table detailing the temperature/time each phase developed when held at 315°C

Sample	Hexagonal $BaCl_2$	Orthorhombic $BaCl_2$	Unknown Phase
JJ194	254/2	315/19	315/11
JJ195	276/4	-	315/10
JJ196	244/3	-	315/5
JJ197	249/4	315/20	315/9
JJ198	273/4	-	315/9
JJ199	246/9	315/6	-

www.manaraa.com

JJ194 heated by ramp, JJ195 315°C isothermal, both JJ196 isothermal scans, JJ198's 325°C isotherm, and JJ199's 315°C isothermal scan developed the unknown phase, and not the orthorhombic $BaCl_2$ phase.

3.1.3 Phosphorimetry (PL)

Phosphorimetry has been shown to indicate the presence of hexagonal and orthorhombic $BaCl_2$ in FCZ glass ceramic samples. Orthorhombic $BaCl_2$ yields an emission peak at apporoximately 402 nm, while hexagonal $BaCl_2$ emits two peaks at aprroximately 410 and 470 nm. Figures 3.5, 3.6, 3.7, 3.8, 3.9, and 3.10 demonstrate that the emission spectra for current and past samples are very similar. Sample JJ124 was previously made and yielded different results than current and other previously made samples; it does not contain $EuCl_2$.

In the emission spectra, samples made to test *in-situ* XRD at Argonne yielded only hexagonal $BaCl_2$ crystals, while other comparison samples yielded the orthorhombic $BaCl_2$. Figure 3.10 demonstrates the anomaly. This is likely due to samples JJ204 and JJ205 containing 3 percent dopants while samples JJ176 and JJ177 contained only 0.8 percent $EuCl_2$.

Phosphorescence that occurs when samples are excited at 360 nm is dependent on the europium in the sample.

Spectra have been stacked for comparison.

3.2 Borate Scintillators

3.2.1 NIST exposure

Samples JJ213, JJ214, JJ215, JJ216, JJ217, and JJ218 in Figure 3.11 are ZBLAN glass ceramics doped with $CeCl_3$ which are not discussed in depth in this thesis. Samples JJ222, JJ223, JJ224, JJ225, and JJ226 in Figure 3.11 are borate silica glass ceramics. Samples JJ222, JJ223, and JJ224 are doped with EuF_2 and yielded the

www.manaraa.com

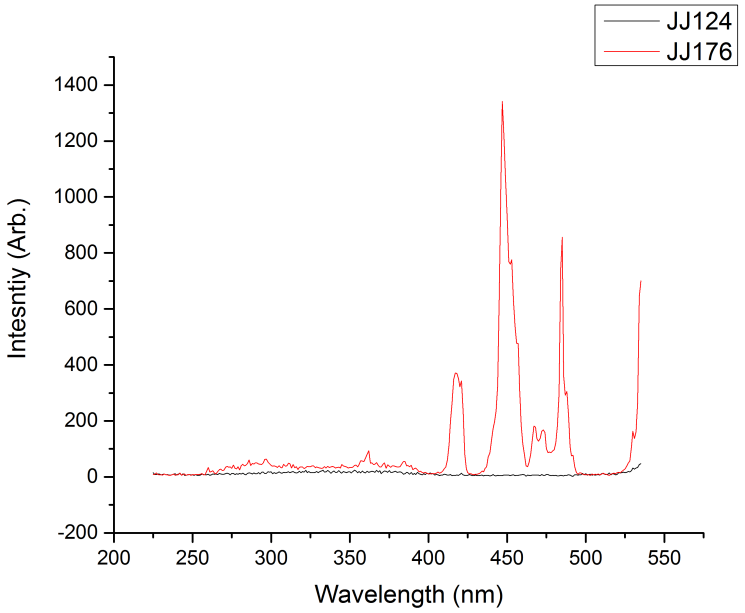

Figure 3.5: Excitation Spectra for previously made FCZ glasses containing 1.2% EuF_2, 0.8% HoF_3 (JJ124) and 0.8%$EuCl_2$ (JJ176). Samples were excited at 545 nm.

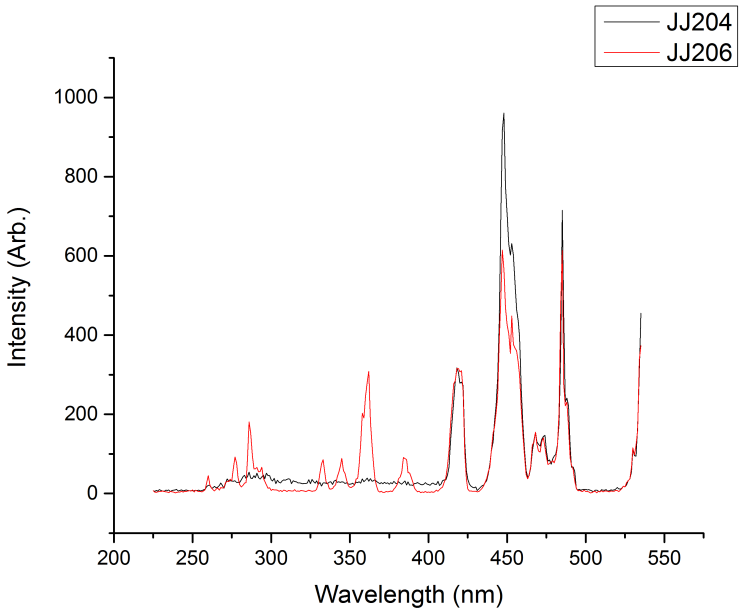

Figure 3.6: Excitation Spectra for FCZ glasses containing 1.5% $EuCl_2$, 1.5% HoF_3 (JJ204) and 3%HoF_3 (JJ206). Samples were excited at 545 nm.

www.manaraa.com

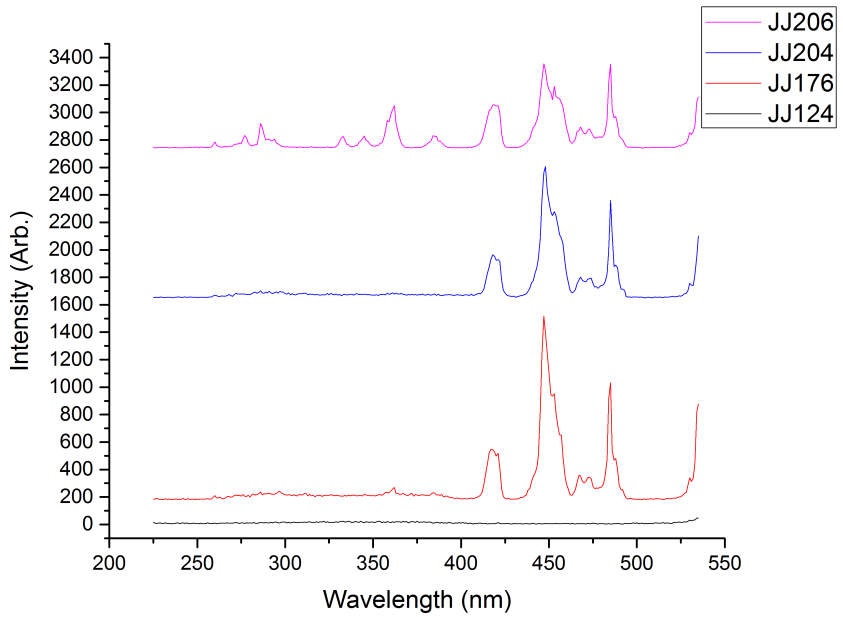

Figure 3.7: Excitation Spectra of samples JJ124, JJ176, JJ204, and JJ206. Samples are stacked for clarity. Samples were excited at 545 nm.

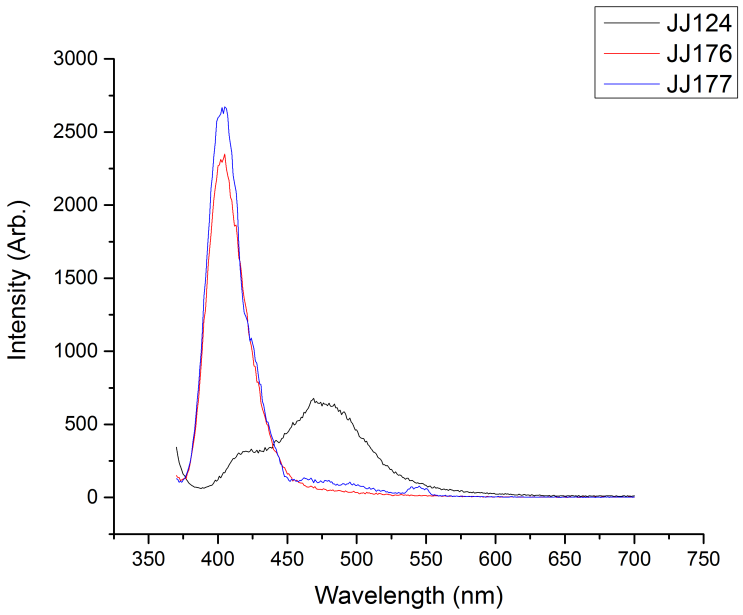

Figure 3.8: Figure 7: Emission spectra for FCZ glasses containing 0.8% EuF_3, 1.2%EuF_2 (JJ124), 0.8% $EuCl_2$ (JJ176), and 0.8% $EuCl_2$, 1.2% HoF_3 (JJ177). The samples were excited at 360 nm.

www.manaraa.com

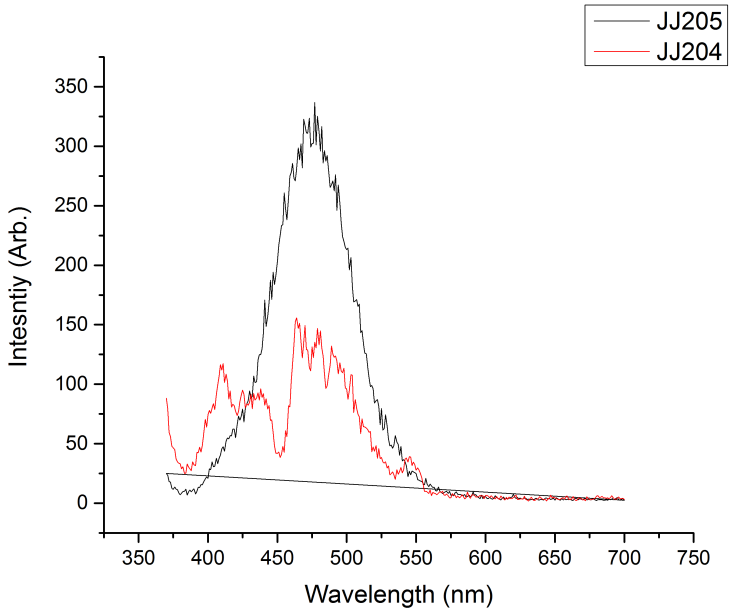

Figure 3.9: Emission spectra for FCZ glasses containing 1.5% $EuCl_2$, 1.5% HoF_3 (JJ204), and 3% $EuCl_2$ (JJ205). The samples were excited at 360 nm.

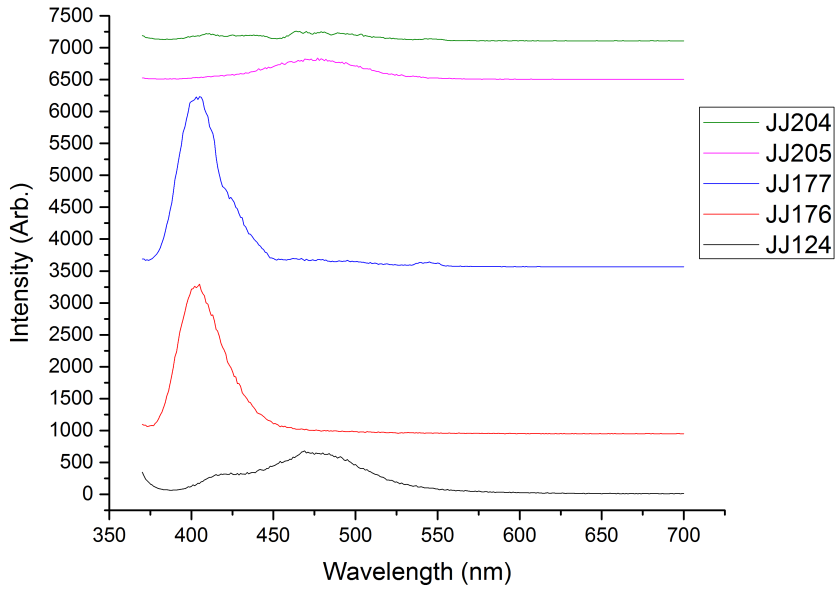

Figure 3.10: Emission spectra for samples JJ124, JJ176, JJ177, JJ204, and JJ205. The samples were excited at 360 nm. The samples were stacked for clarity.

www.manaraa.com

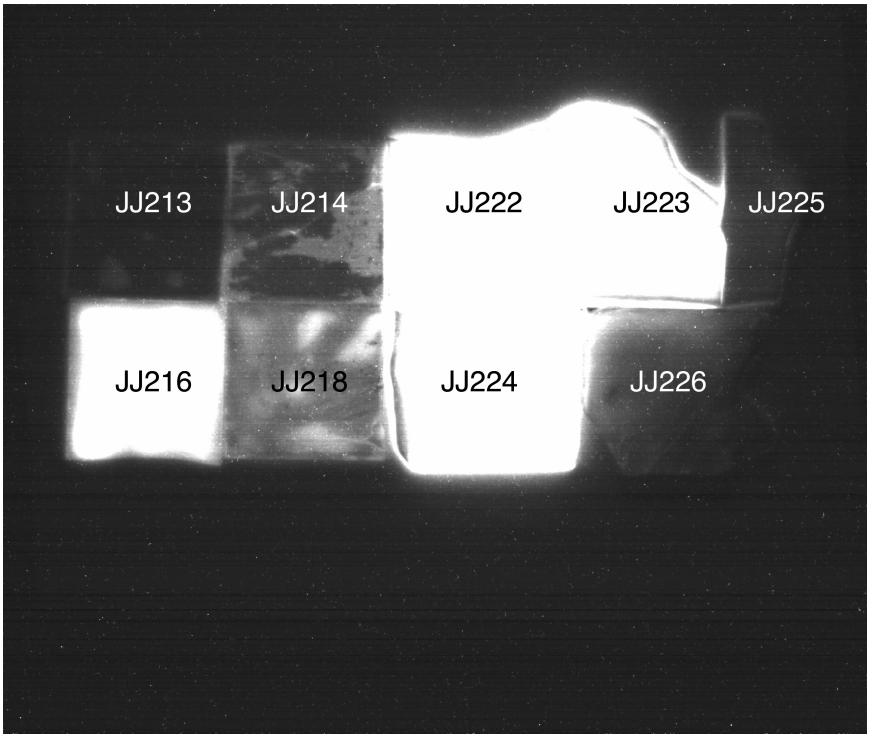

Figure 3.11: Neutron scintillation of "as made" samples

most light output by visible means. Samples JJ225, and JJ226 are doped with $CeCl_3$; they showed no light output. Sample JJ222 does not contain enriched LiF or $^{10}B_2O_3$ like samples JJ223, JJ224, JJ225, and JJ226.

All samples in Figure 3.11 are 1.5 mm thick, and are "as made" in the mold. It is believed that the thickness of these samples contributed to internal light scattering and therefore hindered the light output of the samples. To test this theory, samples JJ223, JJ225, and JJ226 were powdered using a mortar and pestle and attached to the aluminum plate with packaging tape. Figure 3.12 are the images taken of the powdered borated glass ceramic samples. Samples JJ223 and JJ225, which did not show scintillation in Figure 3.11 as 1.5mm thick samples, now show scintillation. Sample JJ225 showed the most improvement in light yield as a thinner sample. The light yield increase of JJ226 is barely detectable.

www.manaraa.com

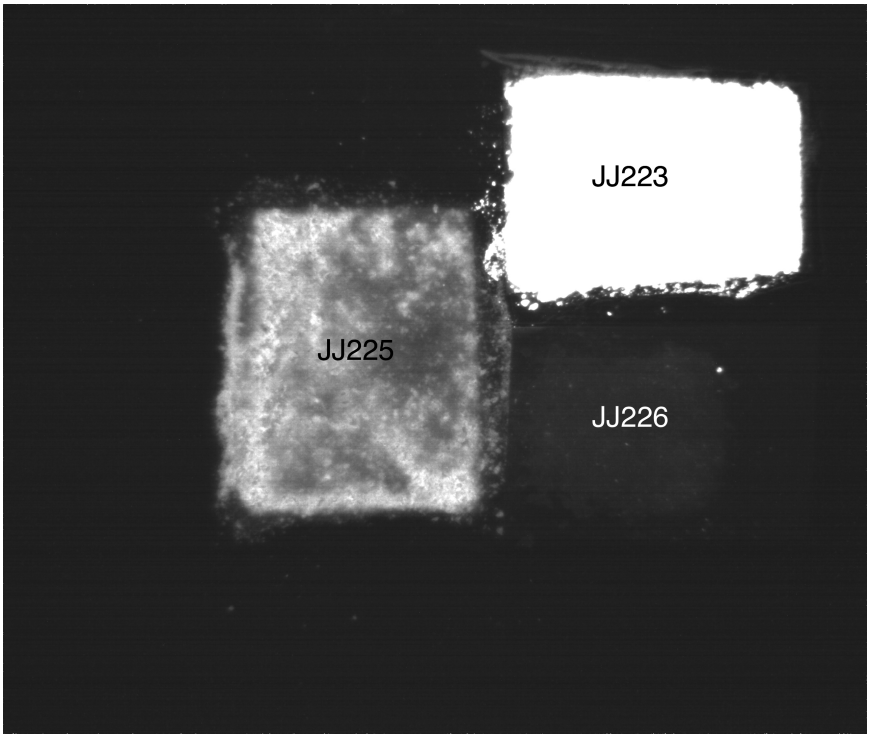

Figure 3.12: Neutron scintillation of powdered LiSiBaB samples

3.2.2 Pulse Height Measurements

After testing at NIST, samples were sent to ORNL for pulse height and pulse shape measurements in order to confirm results obtained at NIST and to test samples that were left out of the NIST experiment.

Pulse height measurements made at Oak Ridge National Lab (ORNL) were done to determine the number of photons per thermal neutron. Sample JJ221 was found to yield the best results as the brightest scintillator. Figure 3.13 below shows the pulse height spectra of JJ221, and Figure 3.14 shows the commercial scintillator GS20 as a reference. The peak position at channel 550 in Figure 3.14 corresponds to 7,000 photons per thermal neutron. For sample JJ221, the peak position at channel 215 corresponds to 2,700 photons per thermal neutron. This is roughly 40 percent of the light output of the commercial GS20 scintillator.

Samples JJ222, JJ224, JJ225, and JJ226 show significantly less light output. Figures 3.15, 3.16, 3.17, 3.18, and 3.19 are the pulse height spectra for samples JJ222,

www.manaraa.com

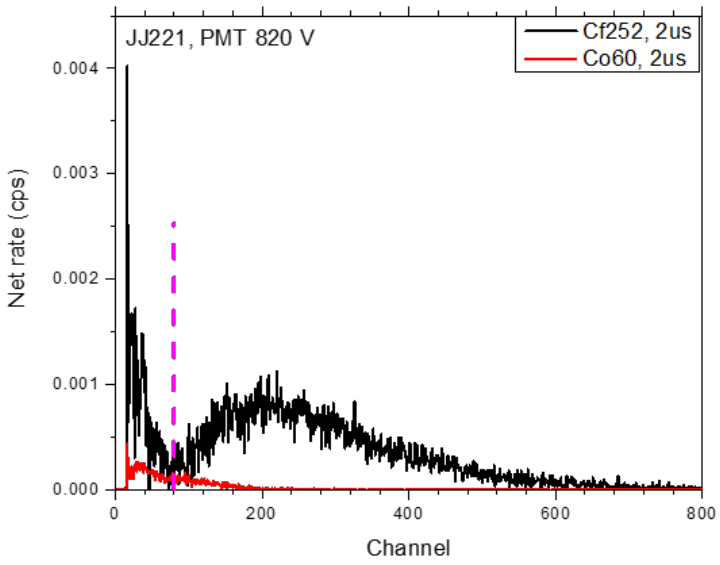

Figure 3.13: Pulse height measurement of sample JJ221

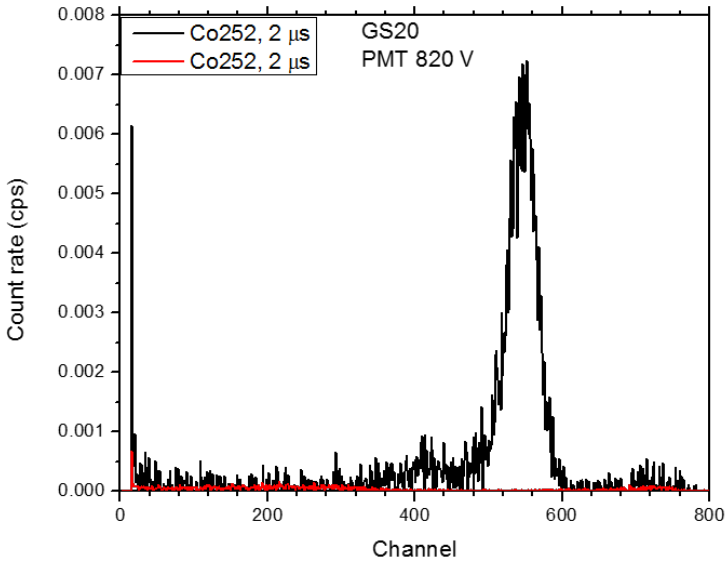

Figure 3.14: Pulse height measurement of the commercial standard GS20

www.manaraa.com

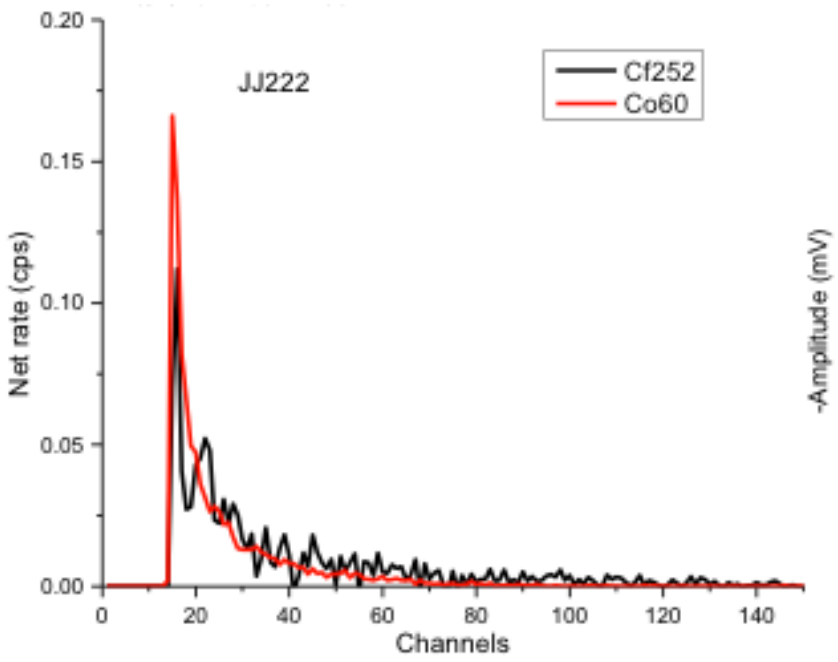

Figure 3.15: Pulse height measurement of sample JJ222

JJ223, JJ224, JJ225, and JJ226 respectively. Note that samples JJ222-JJ226 have no real peak, such as that seen in sample JJ221 and the commercial GS20 scintillator. For the most part, these spectra are just noise, and therefore show no distinct scintillation despite yielding light output at NIST.

3.2.3 Pulse Shape Measurements

Pulse shape measurements performed at ORNL were done to aid in the discrimination between neutrons and gammas. Sample JJ221, which yielded good light output in the pulse shape measurements, also gave comparable results during this experiment. Figure 3.20 seen below is the pulse height spectra for sample JJ221. When compared to Figure 3.21, it is clear that JJ221 shows little difference in the discrimination of neutrons from gamma rays.

www.manaraa.com

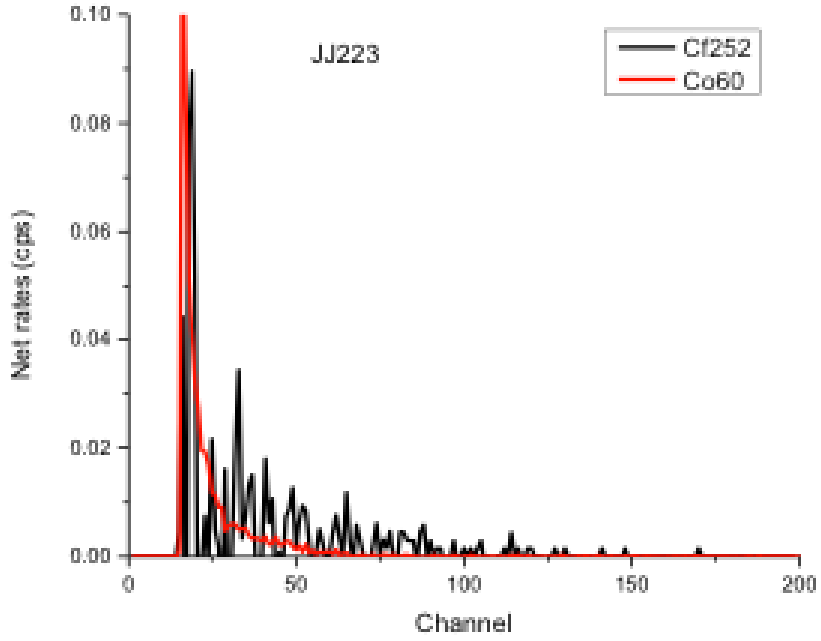

Figure 3.16: Pulse height measurement of sample JJ223

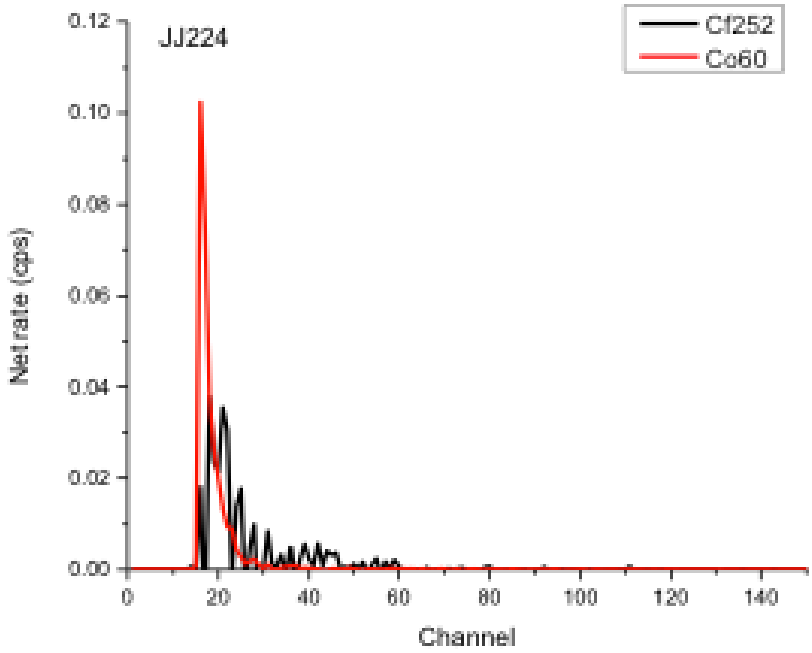

Figure 3.17: Pulse height measurement of sample JJ224

www.manaraa.com

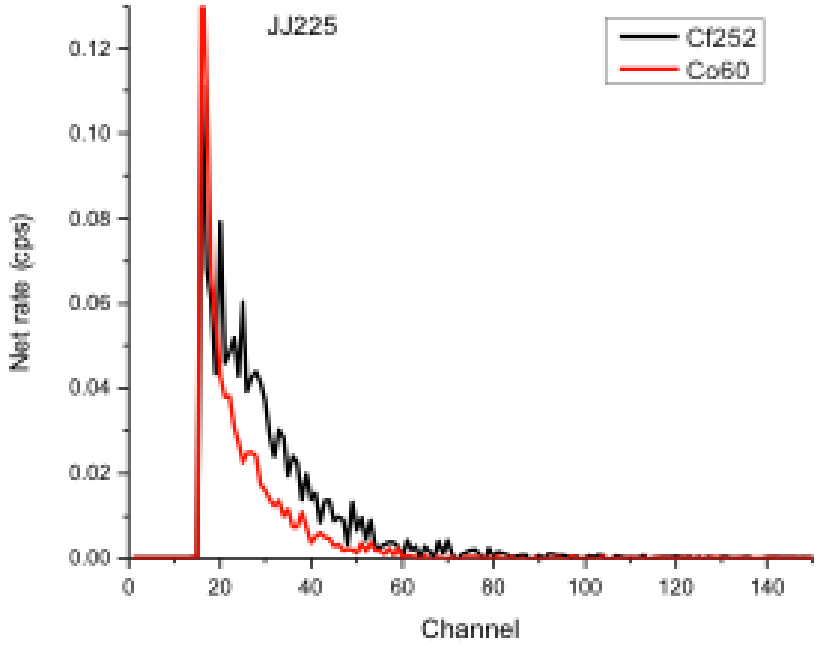

Figure 3.18: Pulse height measurement of sample JJ225

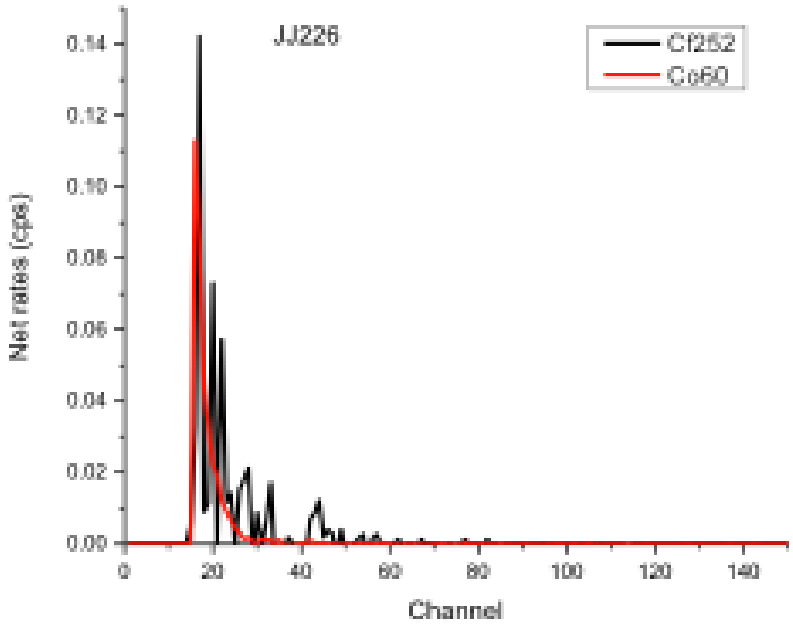

Figure 3.19: Pulse height measurement of sample JJ226

www.manaraa.com

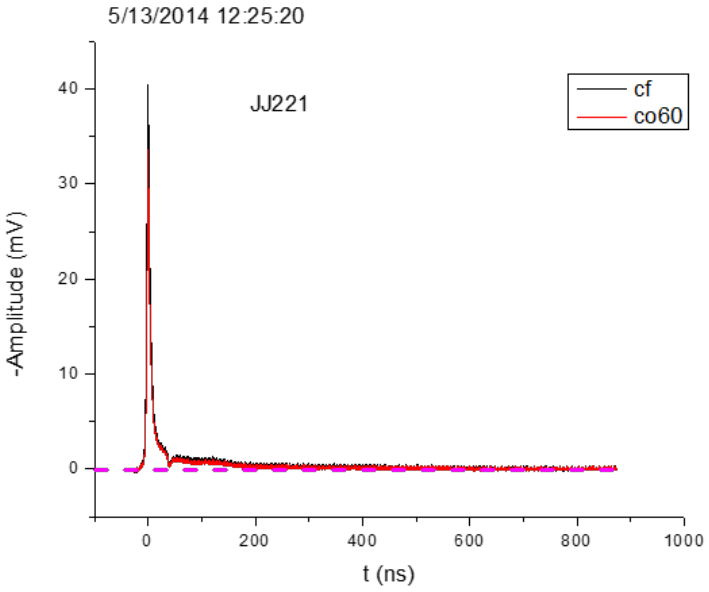

Figure 3.20: Pulse shape measurement of sample JJ221

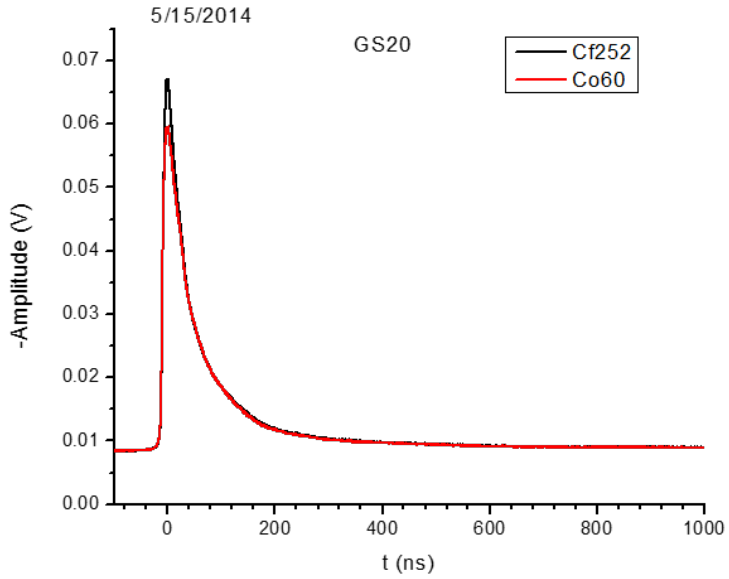

Figure 3.21: Pulse shape measurement of commercial standard GS20

www.manaraa.com

Chapter 4

Conclusions

4.1 ZBLAN Glass Ceramics

Fluorochlorozirconate glass ceramic samples doped with EuF_2, EuF_3, and HoF_3 were produced for use in medical imaging. Samples from previous experiments were replicated in order to duplicate results. Follow up samples were made in an attempt to further improve the efficiency of the glass ceramic as a storage phosphor.

Samples that were repeated with exact compositions yielded different results. The only change made between the old and new experiments was the cleaning procedure. For previously made samples, the platinum crucible used to synthesize the samples was soaked in a borax-water mixture, sanded with fine grit sandpaper to remove remaining contaminants, and finally rinsed with acetone, methanol, and ethanol before being used again. For the new samples, the crucible was soaked in dilute HCl, sanded with fine grit sandpaper to remove any remaining debris, and rinsed with acetone, methanol, and ethanol before use. It is my conclusion that the old cleaning procedure added defects that allowed $BaCl_2$ crystals to form more easily.

An increase in unnecessary dopants (EuF_2, EuF_3, and HoF_3) may aid in the formation of the defects once created by residual borax. New samples with 3% dopants behaved similarly to old samples containing 0.8% dopants. Adding

www.manaraa.com

B_2O_3 (a component of Borax) to the glasses helped to acheive the desired phase transformation.

4.1.1 Future Work

The sample series made with the crucible cleaned in dilute HCl will be optimized to achieve the desired phase and light output. Once optimization is achieved, the unknown phase will be investigated more throughly. The amount of contaminants introduced through the old borax cleaning procedure should be investigated more throughly and the exact amounts contained should be quantitated.

4.2 LiSiBaB Glass Ceramics

Lithium silica barium-boron glass ceramic samples were doped with ^{6}LiF, EuF_2, and $CeCl_3$ in order to create a fast neutron scintillator. Samples doped with EuF_2 containing no enriched isotopes gave the best scintillation results when exposed to thermal neutrons.

Sample JJ221 produced 40% the light output of GS20 (about 2700 photons/neutron). Other samples have much less light output compared to JJ221. Sample JJ221 had no enriched $^{10}B_2O_3$, ^{6}LiF and contained EuF_2 as a dopant rather than $CeCl_3$.

Eliminating enriched isotopes makes these scintillators relatively inexpensive. EuF_2 as a dopant for this glass matrix is new as well. Potential applications for an inexpensive fast scintillator include reactor instrumentation safety (which would ensure containment is working properly in nuclear power and research facilities), transportation safety for detecting neutrons emitted from nuclear materials such as Uranium-233 and plutonium-239 that may be entering the country.

www.manaraa.com

4.2.1 Future Work

Several experiments will follow this work. The glasses should be thinned out to a uniform size of 50.8 x 50.8 x 1 mm. This would match commercial scintillators, such as GS20, and help prevent the internal scattering believed to have been observed in the original thick samples tested at NIST.

The MTF (Modulation Transfer Function) data at knife edges should be captured and analyzed. ICP (Induced Coupled Plasma) should be run to see if ^{6}LiF is still in the enriched samples.

A new sample series based off sample JJ221 should be created in order to optimize its composition. Ideally the samples should be more transparent to aide in the prevention of internal light scattering. These samples will have no $CeCl_3$ or enriched elements (^{6}LiF and $^{10}B_2O_3$) in the new samples series. The samples will be sent to ORNL for quantitative analysis of scintillation.

www.manaraa.com

Bibliography

www.manaraa.com

Anderson, D. (1990). Cerium fluoride: A scintillator for high-rate applications. *Nuclear Instruments and Methods in Physics Research*, 287:606–612. 3

Appleby, B. and Vontobel, P. (2008). Optimisation of lithium borate-barium chloride glass-ceramic thermal neutron imaging plates. *Nuclear Instruments and Methods in Physics Research*, 594:253–256. 2

Appleby, G., Bartle, C., Williams, C., and Edgar, A. (2005). Lithium borate glass ceramics as thermal neutron imaging plates. *Current Applied Physics*, 6:389–192. 2

Carel, W. v. E. (2002). Inorganic scintillators in medical imaging. *Physics in Medicine and Biology*, 47:R85–R106. 3

Gray, S. (2013). An investigation of rare earth co-doping in fluorochlorozirconate glass-ceramic imaging plates to improve the storage phosphor properties for computed radiography. Master's thesis, The University of Tennesse, Knoxville, TN, USA. 2

Mauro, J. and Zanotto, E. (2014). Two centuries of glass research: Historical trends, curent status, and grand challenges for the future. *International Journal of Applied Glass Science*, pages 1–15. 1

Pablick, C. e. a. (2010). Differential scanning calotimetry investigations on eu-doped fluorozirconate-based glass ceramics. *Journal of Non-Crystalline Solids*, 356:3085–3089. 1

www.manaraa.com

Pfau, C. e. a. (2011). Structural phase transitions of barium halide nanocrystals in fluorozirconate glasses studied by raman spectroscopy. *Journal of Applied Physics*, 109:8. 1

Poulain, M. and Soufiane, A. (1992). Fluoride glasses: Synthesis and properties. *Brazilian Journal of Physics*, 22:205–217. 1

Schweizer, S. (2001). Phyics and current understanding of x-ray storage phosphor. *Physica Status Solidi*, 187:335–393. 2

www.manaraa.com

Vita

Julie Swafford was born Julie Elizabeth King in Mount Airy, NC, to Danny and Sandy King. She has a younger brother Jason. She attended Franklin Elementary, Meadowview Middle School and continued to North Surry High School in Mount Airy, North Carolina. After graduation she headed to King College in Bristol, Tennessee to pursue a pre-medical track. At King College she fell in love with Physics and went on to double major in Physics and Mathematics and double minor in Chemistry and Biology. She obtained her Bachelor of Science from King College in December of 2012. She accepted a graduate research assistantship at the University of Tennessee Space Institute in the Biomedical Engineering Department. During her time at the Space Institute, Julie met and married John Mark Swafford. Julie will graduate with a Masters of Science in Biomedical Engineering in December 2014. She will be continuing her education towards a Doctor of Philosophy at The University of Tennessee Space Institute.

www.manaraa.com